

Table ST1: Field site details

Site	WGS84 Approximate center	Elevation (m)	Climate // Vegetation	Mean annual temperature (°C) (PRISM, 1990-2020)	Mean annual precipitation (mm) (PRISM, 1990-2020)
Northernmost	38.0288, -119.1778	2150 – 2500	Semi-arid // sagebrush scrub to piñon/juniper	7.3	407
Middle	36.7189, -118.2408	1400 – 1800	Semi-arid // sagebrush scrub	12.7	265
Southernmost	34.9375, -115.6180	735 - 980	Arid // Creosote bush scrub	18.6	160

Prism database values extracted from 30-year mean maps²⁵.

Table ST2: Power-law trend fits and statistics for fracture metrics over time

Maximum-length fracture growth rate (mm/kyr)					
Site	Rock type	A	k	R ²	Two-tailed p-value
Northernmost	granitoid	63.4	-1.48	0.86	0.07
Middle	granitoid	48.5	-1.09	0.99	0.00
Southernmost	granitoid	31.9	-0.88	1.00	0.00
Southernmost	volcanic	24.0	-0.83	0.60	0.12
Southernmost	carbonate	5.5	-0.38	0.03	0.79
Number density increase rate (fractures/m² per kyr)					
Northernmost	granitoid	<i>Insufficient data for trend fit</i>			
Middle	granitoid	25.11	-0.95	0.99	0.00
Southernmost	granitoid	40.95	-0.97	0.99	0.00
Southernmost	volcanic	42.81	-1.12	0.95	0.01
Southernmost	carbonate	32.35	-0.68	0.29	0.36
Fracture intensity increase rate (mm/m² per kyr)					
Northernmost	granitoid	<i>Insufficient data for trend fit</i>			
Middle	granitoid	990.47	-0.96	0.98	0.00
Southernmost	granitoid	1655.30	-0.95	0.99	0.00
Southernmost	volcanic	1717.90	-1.04	0.78	0.05
Southernmost	carbonate	1014.10	-0.62	0.19	0.47

Power law equation format $y = Ax^k$. Maximum-length fracture growth rate is calculated using the median of all fracture lengths on the modern deposit (0 kyr) and the maximum-length fracture per rock on each dated surface, averaged per surface and rock type.

Figure S1: All fracture plane strikes measured on granitoid rocks on the ~76 kyr exposure age surface at the Middle site. Data are plotted biaxially. Note statistically significant orientations, suggesting a thermal stress origin due to the natural directionality of diurnal solar heating⁵¹.

N fractures = 441;

vector mean = 179° ; median = 5° ; circular std. dev. = 64° ;

Rayleigh p-value = 0.05; Rao's spacing p-value = <0.01

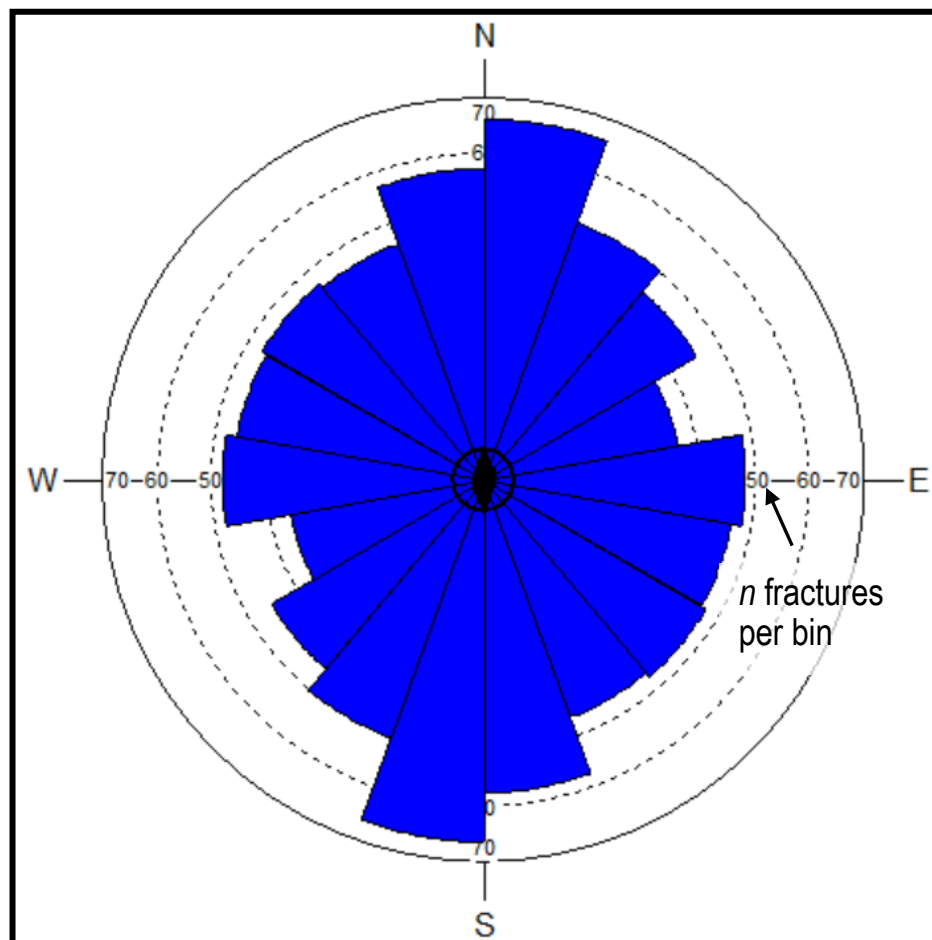


Figure S2: A. Northernmost site modern creek deposit with measurement boulders on a small unvegetated bar adjacent to the active channel. **B.** typical Middle site modern boulder bar with measuring tape indicating transect measurement location. **C.** Southernmost site modern boulder bar exhibiting impact marks and minimal varnish, lichen, and fractures.

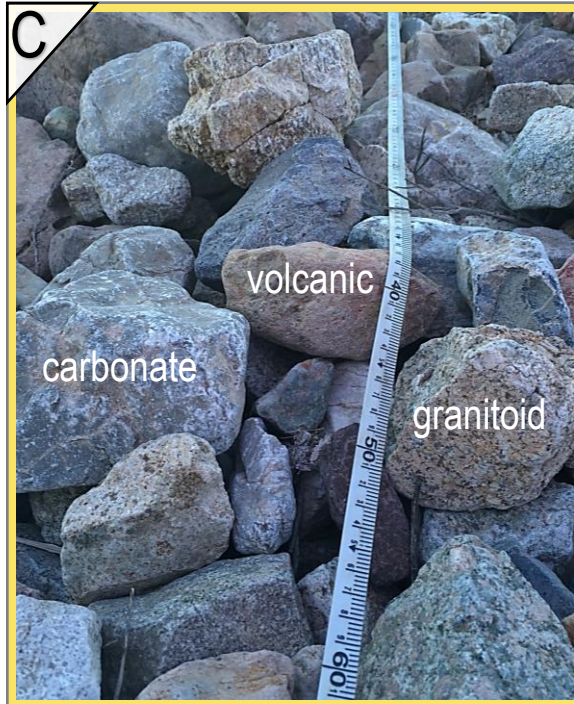


Figure S3: Depositional surfaces on which boulders were measured, with ages in kyr before present. Notice difference in abundance and type of vegetation at Northernmost (coolest, present day semi-arid), Middle (warmer, semi-arid), and Southernmost (hot, arid) sites, reflecting increasing aridity from North to South.

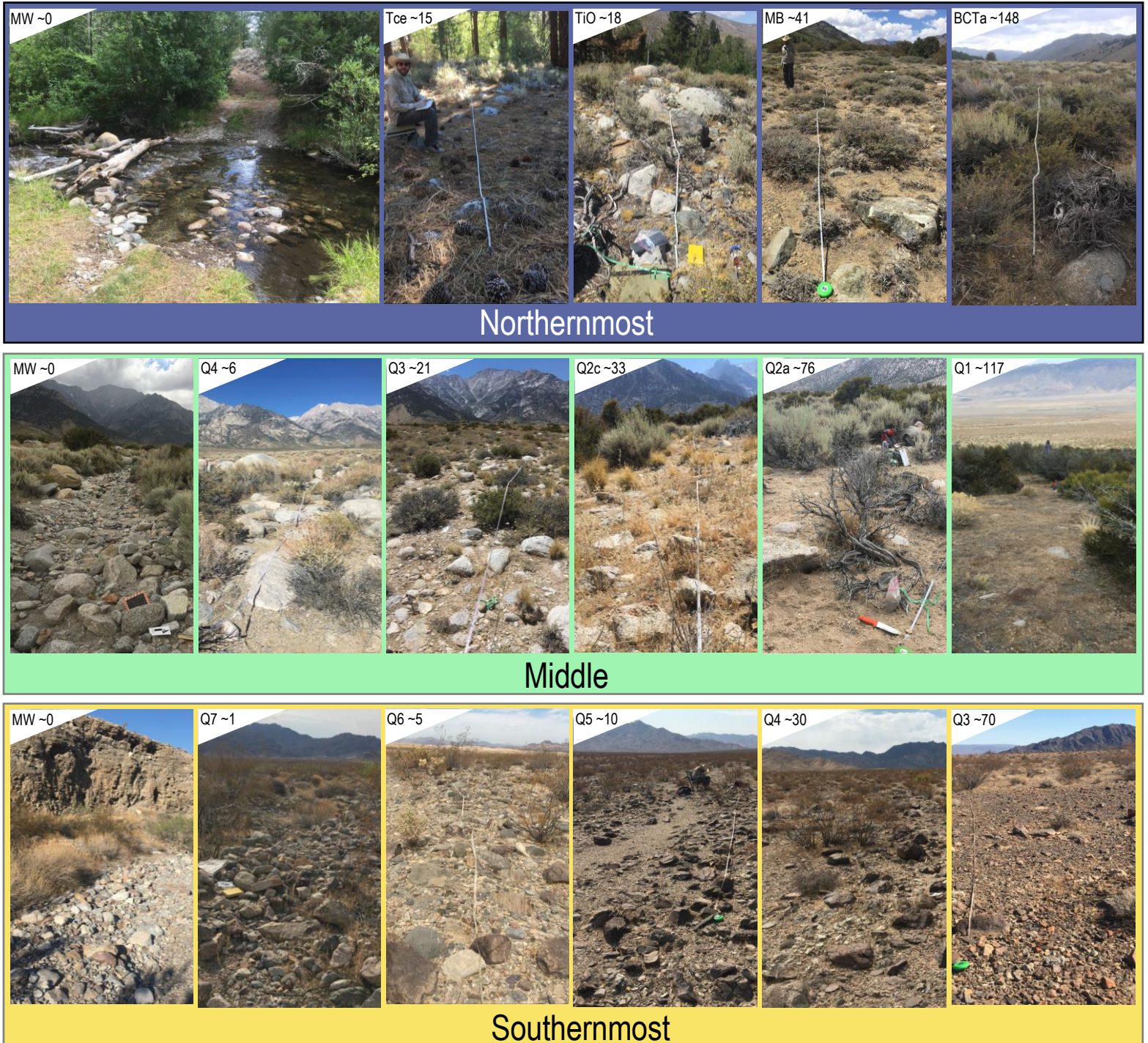


Figure S4: Thin section analyses from select samples of the Middle site. **A.** Thin section of a granite sample. **B.** Microstructure scanned by microscopy and **C.** the same sample as B, showing the mapped fractures isolated for import into FracPaQ to analyze fracture properties. Microcracking chronofunctions of **D.** number density and **E.** intensity derived from 3-5 locations within thin sections of selected rocks of identical lithology from the Intermediate site.

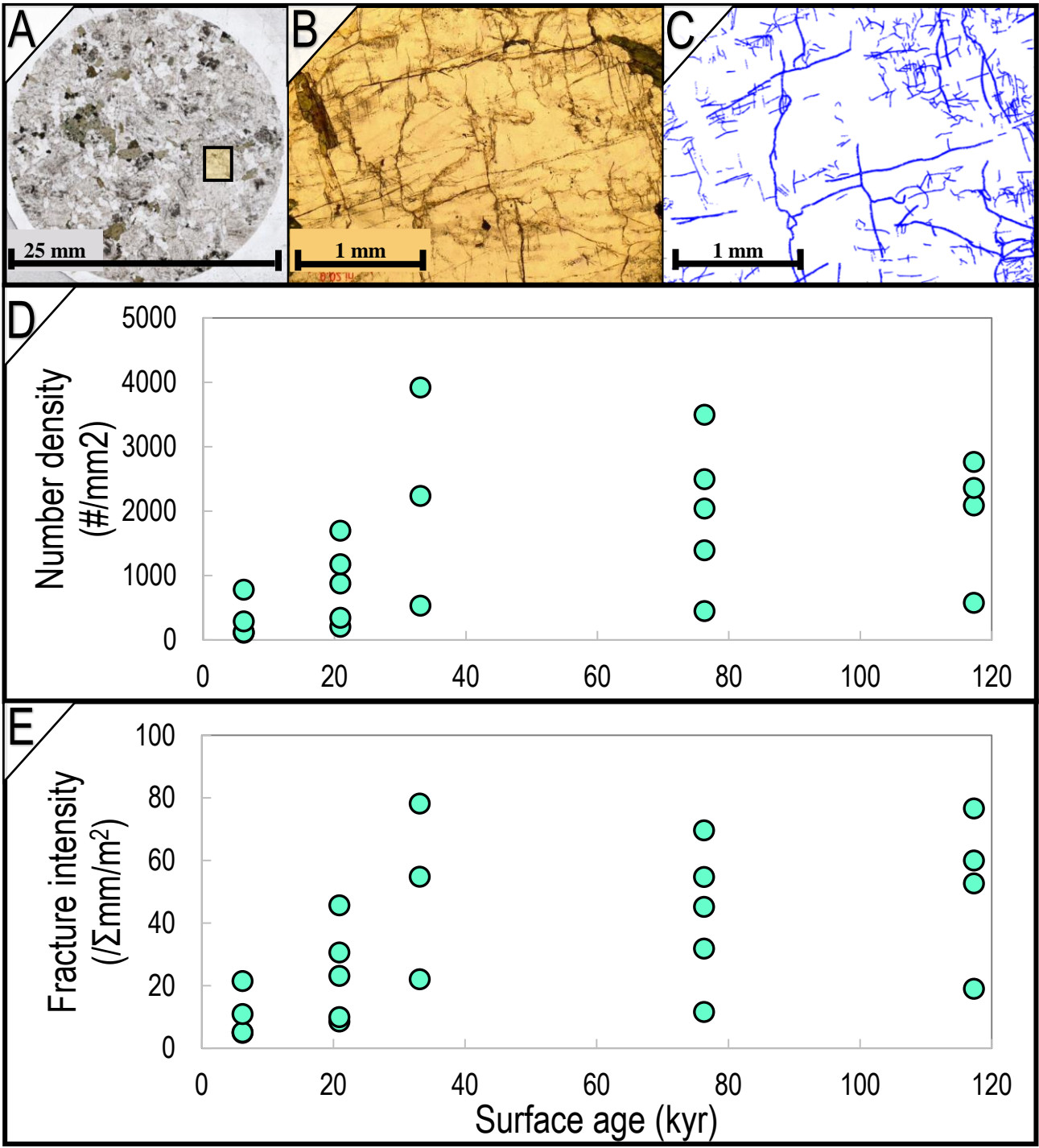


Figure S5: A. Exponential distribution of fractures (length vs. count) from 90 randomly selected granitoid clasts per surface at the Middle site. Y-axis displays the number of all cracks counted within a given 5mm bin on each surface. Surface bars are non-normalized and overlapped, indicating that the modern surface (0 ka) has the least cracks overall. **B.** Probability that a rock will contain fractures of a given length or longer, calculated using the inset equation and all fractures on all rocks measured at the Middle site. The exceedance probability function exhibits similar distributions for the 0, 6, and 21 kyr surfaces; then higher probabilities of longer fractures on the next older 33 and 76 kyr surfaces. The 117 kyr surface data (the oldest rocks) indicate that fracture length probabilities have “reset” to initial values, although the histogram (A) shows that these rocks still have a higher number of fractures than the modern (0 kyr) rocks.

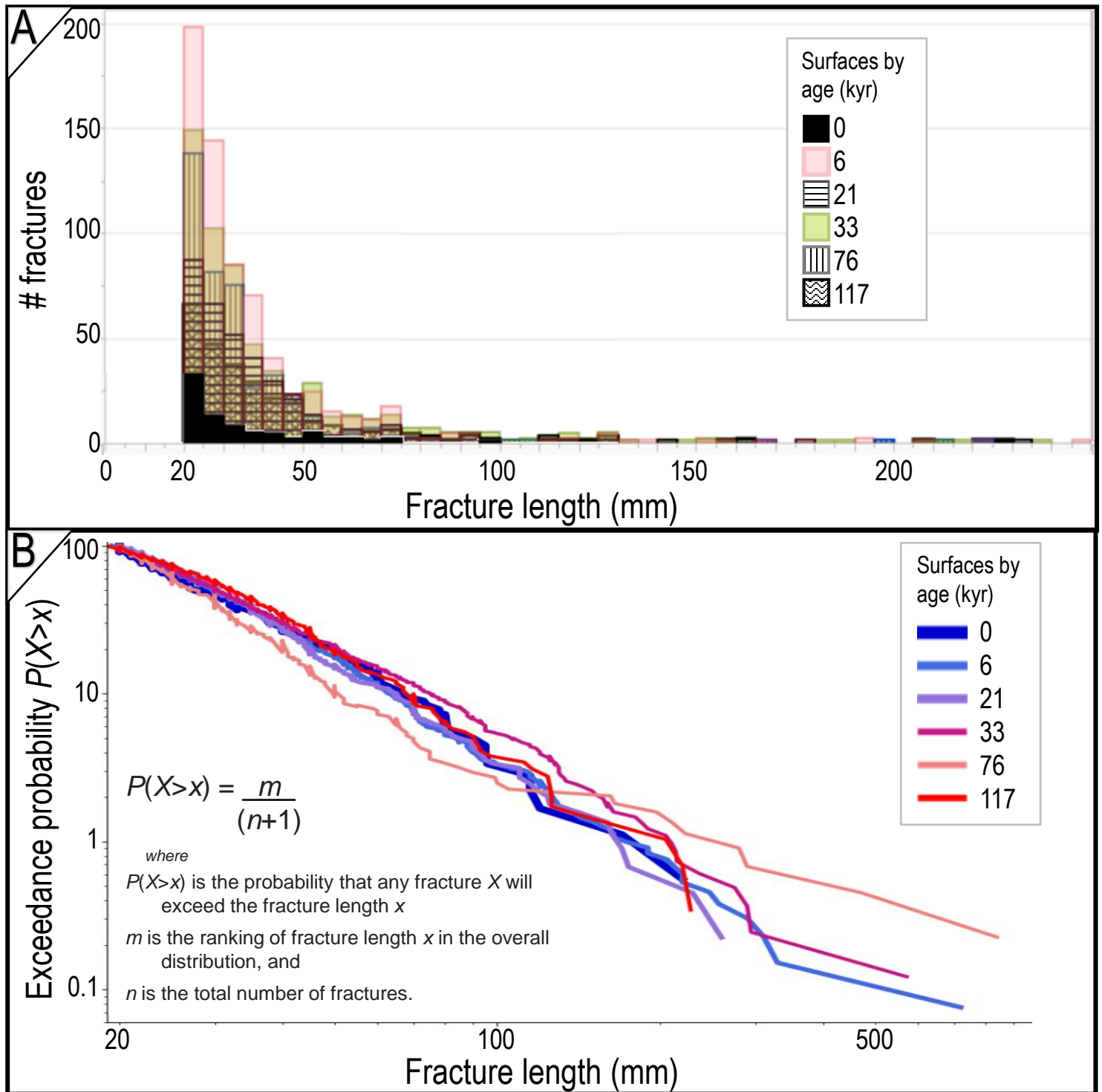


Figure S6: Wolman pebble counts collected at regular intervals along each bar surface, represented as normalized histograms of the relative count of each rock size bin, with surface ages in kyr overlain to the right of each distribution. Three primary axes were measured on every ≥ 10 mm intermediate axis length granitoid clast encountered at the **A. Middle site, granitoid rocks, and B.-D. Southernmost site granitoid, volcanic, and carbonate rocks.** Displayed data are 10 mm bins of long-axis length of clasts. Dark bars represent means.

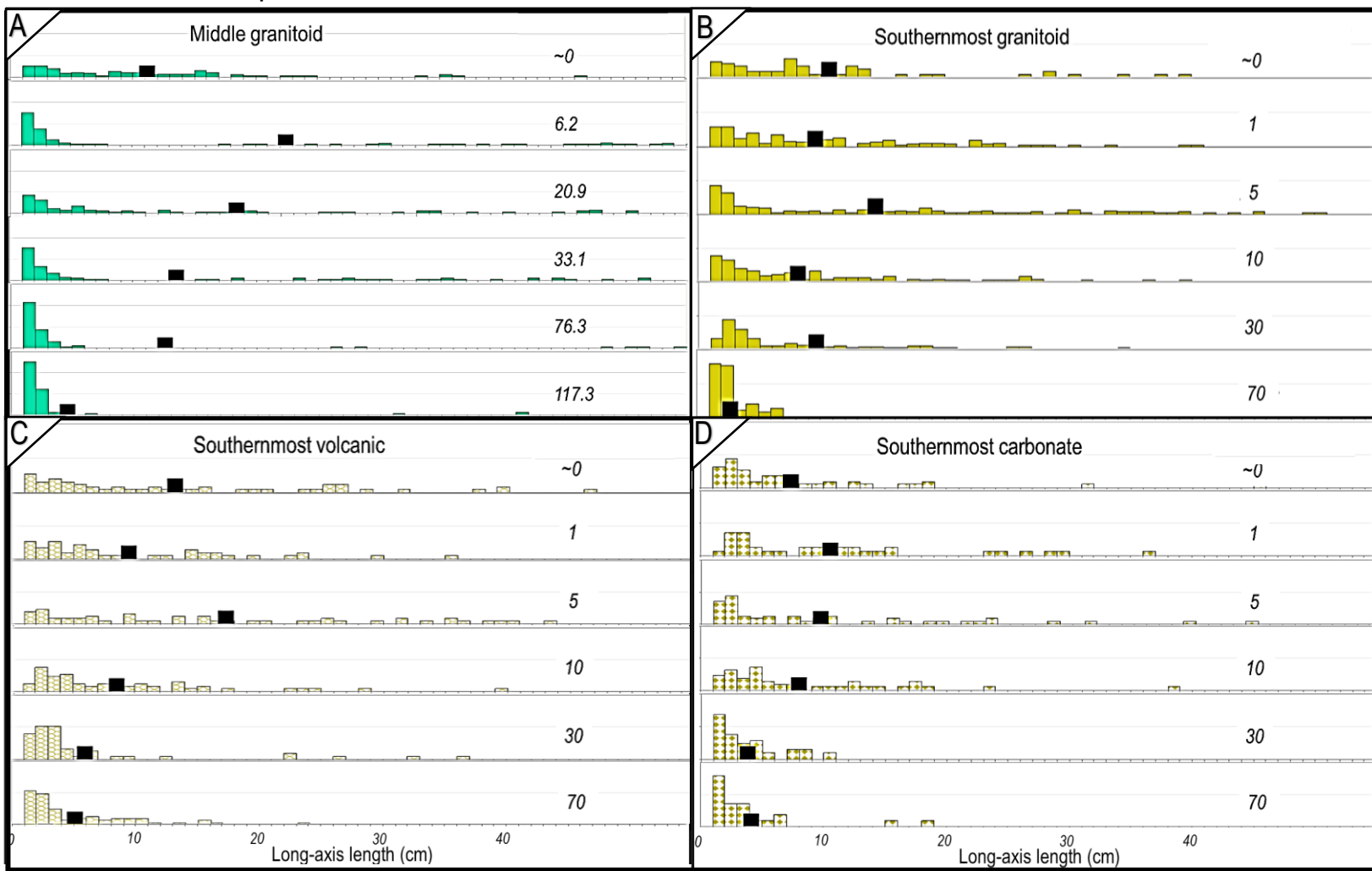


Figure S7: A. Maximum-length fractures and **B.** maximum-length fracture growth rates for smaller rocks (left) vs. rates for larger rocks (right). Cut-off of rock sizes was 30 cm long-axis length for the Northernmost and Middle site and 20 cm long-axis length at the Southernmost site, where rocks were smaller overall. Negative points exist where 1) large volcanic rocks at the Southernmost site are estimated to *decrease* in length by -4 mm/kyr on the 1 kyr surface; and 2) large and small granitoid rocks at the Northernmost site are near-zero and/or negative on the two oldest surfaces. Negative points were not included in trendline fitting.

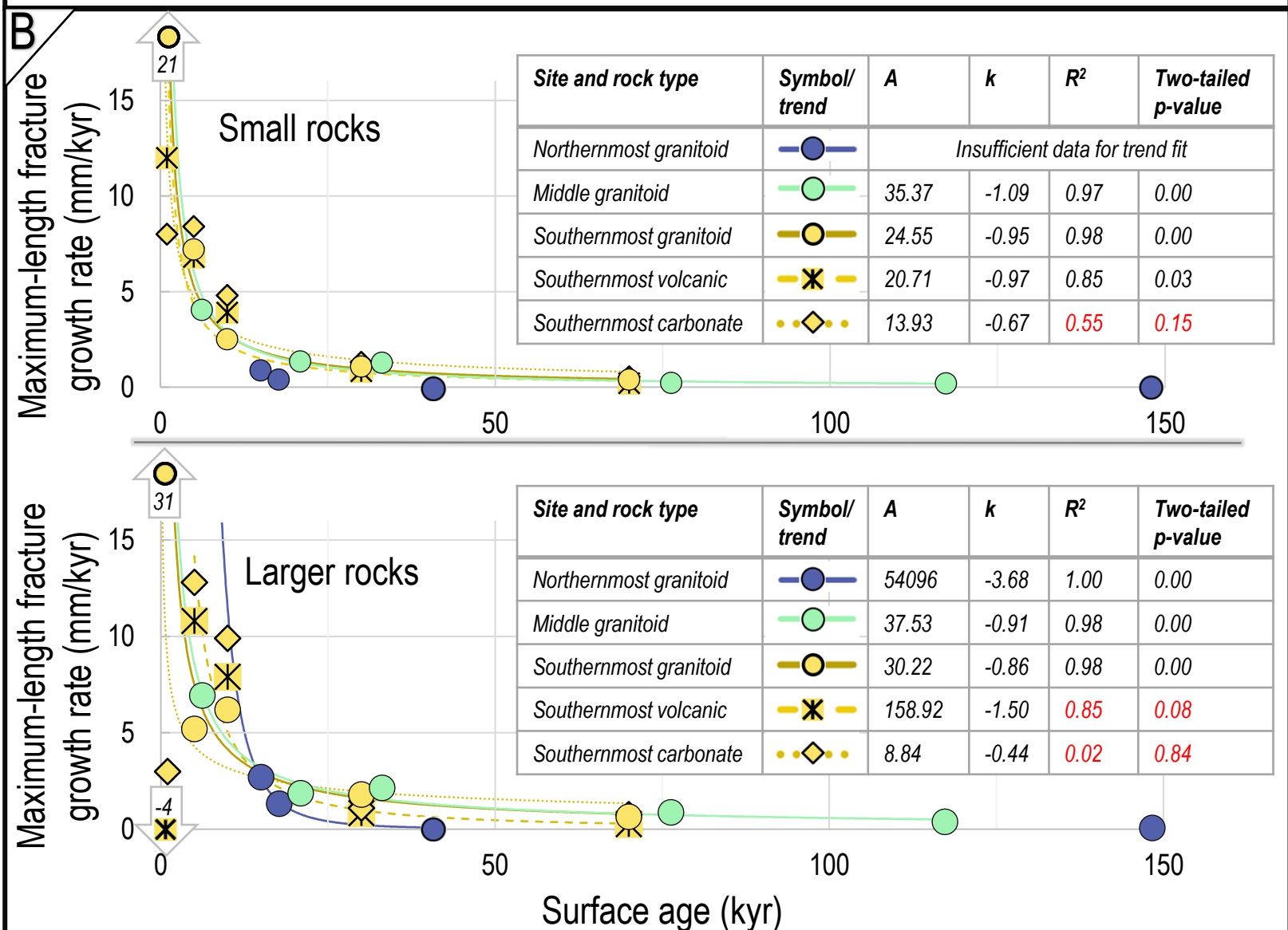
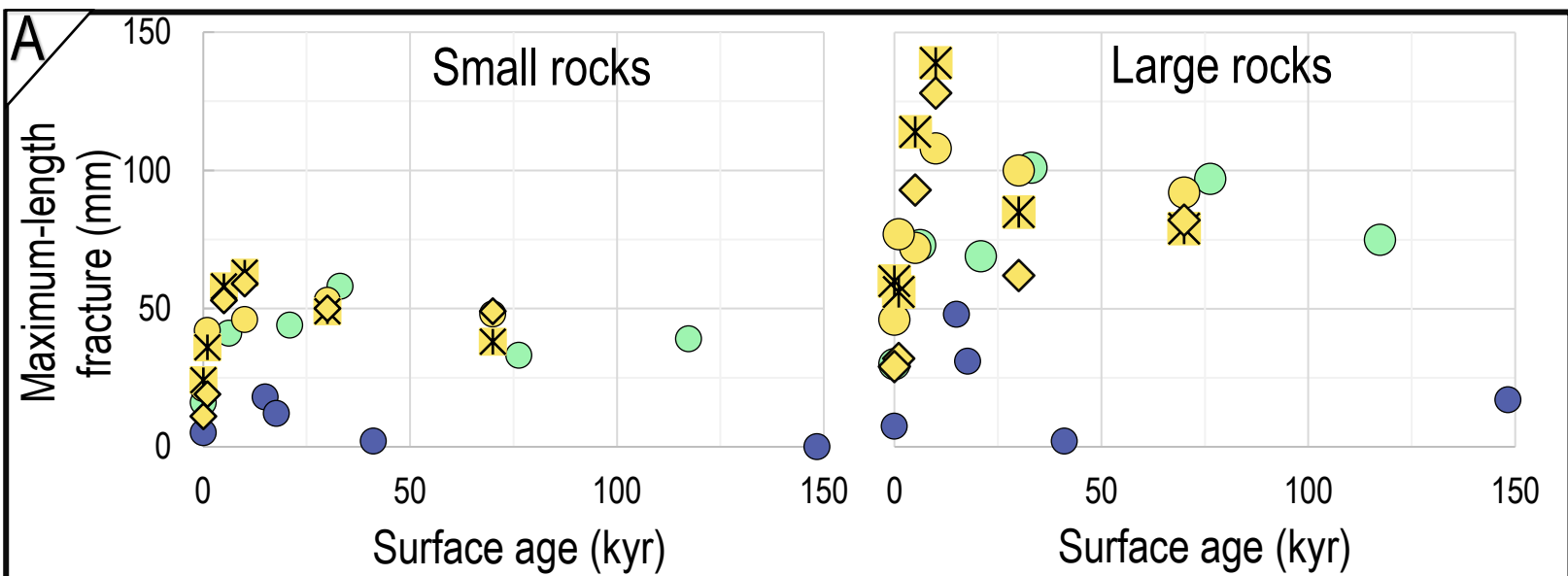


Figure S8: A. Grain size and **B.** mafic mineral percentages of Middle site granitoid rocks. Solid circles represent mean value and horizontal lines of boxes indicate p25, p50, and p75 percentiles. Whiskers represent outlier extents. The Middle site contains the highest number of boulders measured and therefore the most statistically robust subsets of data. The lack of time trends suggest that the observed and calculated cracking metrics are not artifacts of “survivor’s bias” due to exceptional rocks remaining on older surfaces.

